



Short communication

An amorphous $\text{LiCo}_{1/3}\text{Mn}_{1/3}\text{Ni}_{1/3}\text{O}_2$ thin film deposited on NASICON-type electrolyte for all-solid-state Li-ion batteries

J. Xie^{a,b,*}, N. Imanishi^a, T. Zhang^a, A. Hirano^a, Y. Takeda^a, O. Yamamoto^a^a Department of Chemistry, Faculty of Engineering, Mie University, 1577 Kurimamachiya-cho, Tsu, Mie 514-8507, Japan^b Department of Materials Science and Engineering, Zhejiang University, Hangzhou 310027, China

ARTICLE INFO

Article history:

Received 18 January 2010

Received in revised form 10 March 2010

Accepted 10 March 2010

Available online 17 March 2010

Keywords:

Amorphous $\text{LiCo}_{1/3}\text{Mn}_{1/3}\text{Ni}_{1/3}\text{O}_2$ thin film

Cathode material

 $\text{Li}_{1+x+y}\text{Al}_x\text{Ti}_{2-x}\text{Si}_y\text{P}_{3-y}\text{O}_{12}$

All-solid-state Li-ion batteries

Radio frequency magnetron sputtering

ABSTRACT

Amorphous $\text{LiCo}_{1/3}\text{Mn}_{1/3}\text{Ni}_{1/3}\text{O}_2$ thin films were deposited on the NASICON-type Li-ion conducting glass ceramics, $\text{Li}_{1+x+y}\text{Al}_x\text{Ti}_{2-x}\text{Si}_y\text{P}_{3-y}\text{O}_{12}$ (LATSP), by radio frequency (RF) magnetron sputtering below 130°C . The amorphous films were characterized by X-ray diffraction (XRD) and scanning electron microscopy (SEM). The $\text{Li}/\text{PEO}_{18}\text{-Li}(\text{CF}_3\text{SO}_2)_2\text{N}/\text{LATSP}/\text{LiCo}_{1/3}\text{Mn}_{1/3}\text{Ni}_{1/3}\text{O}_2/\text{Au}$ all-solid-state cells were fabricated to investigate the electrochemical performance of the amorphous films. It was found that the low-temperature deposited amorphous cathode film shows a high discharge voltage and a high discharge capacity of around 130 mAh g^{-1} .

© 2010 Elsevier B.V. All rights reserved.

1. Introduction

In recent years, there is an increasing need for the all-solid-state microbatteries due to the rapid development of microelectronics devices. The thin film Li-ion battery is one of the best choices as power source for these devices. The findings of some inorganic solid electrolytes with a high Li-ion conductivity, such as $\text{Li}(\text{P,N})\text{O}_3$ (Lipon) [1–3], NASICON-type glass ceramics [4,5], LVSO [6,7], and LLT [8,9], make it possible for the fabrication of all-solid-state Li-ion batteries. Among them, the NASICON-type electrolyte, $\text{Li}_{1+x}\text{M}_x\text{Ti}_{2-x}(\text{PO}_4)_3$, has been received great interest because of its high Li-ion conductivity at room temperature. Recently, all-solid-state Li-batteries based on this electrolyte have been cycled successfully at room temperature [10,11].

However, the as-obtained cathode films by sputtering are generally amorphous or partially crystalline if the substrate is not preheated. Low capacity and low operating voltage are always observed for these amorphous films compared with the crystalline films [12–15]. Therefore, preheating the substrate or post-annealing the film is necessary to improve the crystallization of the films. However, these processes are complicate for the preparation of the microbatteries and cause some undesired side reactions

[16,17]. In this work, amorphous $\text{LiCo}_{1/3}\text{Mn}_{1/3}\text{Ni}_{1/3}\text{O}_2$ thin films were prepared on the NASICON-type $\text{Li}_{1+x+y}\text{Al}_x\text{Ti}_{2-x}\text{Si}_y\text{P}_{3-y}\text{O}_{12}$ (LATSP) substrates by radio frequency (RF) magnetron sputtering at low-temperature (not over 130°C). The as-prepared amorphous film exhibits a high discharge voltage and a high specific capacity. The results show that the fabrication process of the microbatteries can be significantly simplified when amorphous $\text{LiCo}_{1/3}\text{Mn}_{1/3}\text{Ni}_{1/3}\text{O}_2$ thin films are used directly.

2. Experimental

The glass ceramics plates, LATSP (0.26 mm in thickness), provided by OHARA Inc., were used as the solid electrolyte for the following experiments, the conductivity of which was about 10^{-4} S cm^{-1} at room temperature. $\text{LiCo}_{1/3}\text{Mn}_{1/3}\text{Ni}_{1/3}\text{O}_2$ powder was prepared by two-step solid-phase reactions using stoichiometric amount of $\text{Li}(\text{OCOCH}_3)_2\cdot 2\text{H}_2\text{O}$, $\text{Co}(\text{OCOCH}_3)_2\cdot 4\text{H}_2\text{O}$, $\text{Mn}(\text{OCOCH}_3)_2\cdot 4\text{H}_2\text{O}$ and $\text{Ni}(\text{OCOCH}_3)_2\cdot 4\text{H}_2\text{O}$ as the starting materials. The mixture was pressed into pellets and heated at 400°C for 5 h. The reaction product was then ground and pressed again into pellets, and headed at 900°C for 20 h. The $\text{LiCo}_{1/3}\text{Mn}_{1/3}\text{Ni}_{1/3}\text{O}_2$ thin films (8 mm × 8 mm) were deposited on the LATSP substrates (10 mm × 10 mm) by RF magnetron sputtering using an Ulvac SCOTT-C3. The target (50 mm in diameter) used for sputtering was prepared by cold pressing the $\text{LiCo}_{1/3}\text{Mn}_{1/3}\text{Ni}_{1/3}\text{O}_2$ powder. The $\text{LiCo}_{1/3}\text{Mn}_{1/3}\text{Ni}_{1/3}\text{O}_2$ sputtering was carried out for 2 h in an Ar/O_2 mixture (30% O_2) or pure Ar with a total pressure of 2 Pa and a power of 50 W. The weight of the film was calculated by

* Corresponding author at: Department of Materials Science and Engineering, Zhejiang University, Hangzhou 310027, China. Tel.: +86 571 87951203; fax: +86 571 87951451.

E-mail address: xiejian1977@zju.edu.cn (J. Xie).

the weight gain of the substrate before and after sputtering using a precise balance. The substrate with an aluminium mask was placed 10 cm away from the target. Au film was then deposited on the $\text{LiCo}_{1/3}\text{Mn}_{1/3}\text{Ni}_{1/3}\text{O}_2$ by RF magnetron sputtering from an Au target in pure Ar for 30 min as a current collector to form a LATSP/ $\text{LiCo}_{1/3}\text{Mn}_{1/3}\text{Ni}_{1/3}\text{O}_2$ /Au electrode. For comparison, the $\text{LiCo}_{1/3}\text{Mn}_{1/3}\text{Ni}_{1/3}\text{O}_2$ films were also sputtered on Au substrates under the same conditions to form $\text{LiCo}_{1/3}\text{Mn}_{1/3}\text{Ni}_{1/3}\text{O}_2$ /Au electrodes. The as-prepared electrodes were then post-annealed in air for 0.5 h. The crystalline structure of the films was characterized by X-ray diffraction (XRD) using a RINT2000/PC diffractometer with $\text{Cu K}\alpha$ radiation. The surface and cross-sectional morphologies of the films were observed by scanning electron microscopy (SEM) using a Hitachi S-4000. The chemical composition of the film was determined by inductively coupled plasma (ICP) spectroscopy using a Shimadzu ICPS-1000IV spectrometer.

$\text{Li}/\text{PEO}_{18}\text{-Li}(\text{CF}_3\text{SO}_2)_2\text{N}/\text{LATSP}/\text{LiCo}_{1/3}\text{Mn}_{1/3}\text{Ni}_{1/3}\text{O}_2/\text{Au}$ cells were fabricated to investigate the electrochemical performance of the $\text{LiCo}_{1/3}\text{Mn}_{1/3}\text{Ni}_{1/3}\text{O}_2$ thin films. A polyethyleneoxide (PEO)-based solid polymer electrolyte film, $\text{PEO}_{18}\text{Li}(\text{CF}_3\text{SO}_2)_2\text{N}$, was inserted between Li and LATSP to prevent the reactions between Li and LATSP. The polymer electrolyte was prepared by our previously reported method [18]. Galvanostatic cycling of the cells was carried out at $5 \mu\text{A}$ ($7.8 \mu\text{A cm}^{-2}$) between 2.5 and 4.5 V. Electrochemical impedance spectroscopy (EIS) measurement was conducted by applying an ac signal of 10 mV amplitude over the frequency range from 1 MHz to 1 mHz using a Solartron 1287 electrochemical interface combined with a Solartron 1260 frequency response analyzer. The EIS plots were recorded at the open circuit voltages of about 3.4 V. For comparison, Li/liquid

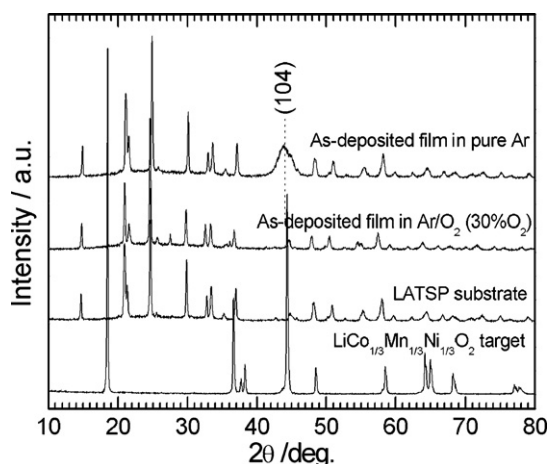


Fig. 1. XRD patterns of the as-deposited $\text{LiCo}_{1/3}\text{Mn}_{1/3}\text{Ni}_{1/3}\text{O}_2$ thin films on LATSP.

electrolyte/ $\text{LiCo}_{1/3}\text{Mn}_{1/3}\text{Ni}_{1/3}\text{O}_2$ /Au cells were also fabricated and cycled at $5 \mu\text{A}$ between 2.5 and 4.5 V. The liquid electrolyte used was 1 M LiClO_4 in a mixture of ethylene carbonate and diethylene carbonate (1:1 in volume). All the electrochemical measurements were performed at 50°C .

3. Results and discussion

Fig. 1 shows the XRD patterns of the $\text{LiCo}_{1/3}\text{Mn}_{1/3}\text{Ni}_{1/3}\text{O}_2$ thin films deposited on the LATSP substrates. The XRD patterns of the

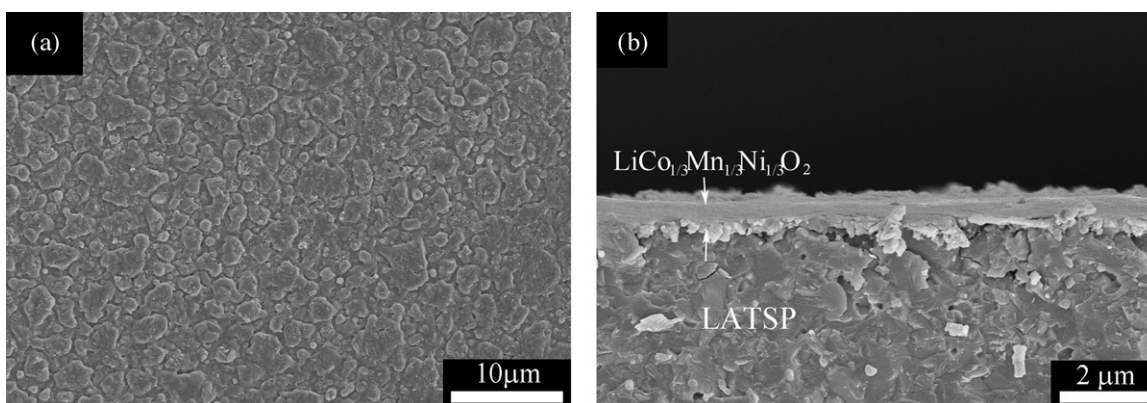


Fig. 2. SEM images of the as-deposited $\text{LiCo}_{1/3}\text{Mn}_{1/3}\text{Ni}_{1/3}\text{O}_2$ thin films on LATSP in Ar/O_2 (30% O_2): (a) surface and (b) cross-section.

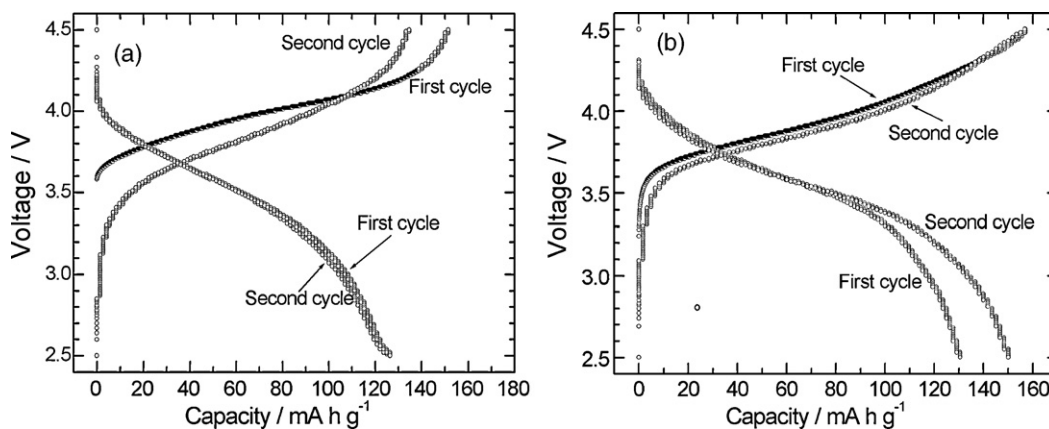


Fig. 3. Voltage profiles of (a) the as-deposited and (b) the 500°C -annealed $\text{LiCo}_{1/3}\text{Mn}_{1/3}\text{Ni}_{1/3}\text{O}_2$ thin films deposited on the solid electrolyte (LATSP) in Ar/O_2 (30% O_2). The curves were recorded between 2.5 and 4.5 V at a current density of $7.8 \mu\text{A cm}^{-2}$.

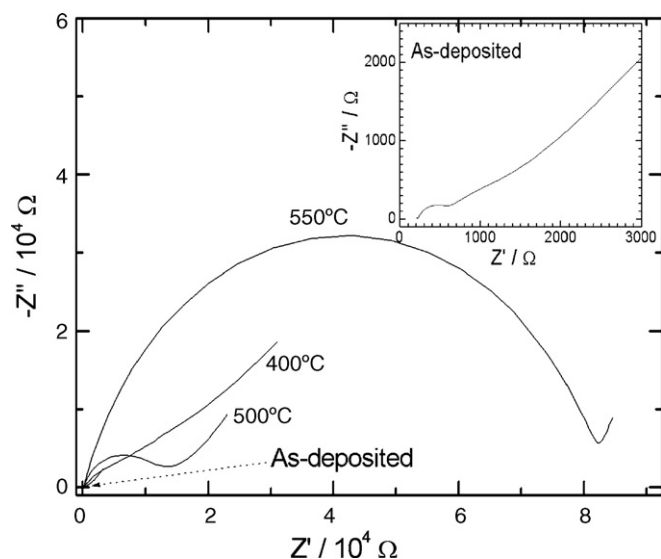


Fig. 4. Nyquist plots of the $\text{LiCo}_{1/3}\text{Mn}_{1/3}\text{Ni}_{1/3}\text{O}_2$ thin films prepared on LATSP in Ar/O_2 (30% O_2) annealed at various temperatures recorded at the open circuit voltages of about 3.4 V.

$\text{LiCo}_{1/3}\text{Mn}_{1/3}\text{Ni}_{1/3}\text{O}_2$ target agree well with the previous reports [19,20]. No peak attributed to $\text{LiCo}_{1/3}\text{Mn}_{1/3}\text{Ni}_{1/3}\text{O}_2$ can be found in the as-deposited thin film in Ar/O_2 (30% O_2). In contrast, the film deposited in pure Ar exhibits a partially crystalline structure with a (1 0 4) preferred orientation at diffraction angle about 44° (2θ). The ICP analysis shows that the molar ratio of Li:Co:Mn:Ni of the as-deposited thin film on Au is 1:0.31:0.27:0.26. Note that the content of Li is slightly rich. For simplicity, $\text{LiCo}_{1/3}\text{Mn}_{1/3}\text{Ni}_{1/3}\text{O}_2$ is still used in the following sections. It was found that the thin films deposited both in pure Ar and in $\text{Ar} + 30\% \text{O}_2$ showed improved crystallization upon annealing at high-temperatures, but annealing also results in the reactions between film and the LATSP.

Fig. 2 shows the SEM images of the as-deposited $\text{LiCo}_{1/3}\text{Mn}_{1/3}\text{Ni}_{1/3}\text{O}_2$ thin film on the LATSP prepared in Ar/O_2 (30% O_2). As seen in Fig. 2(a), the surface of the film is coarse with some islands, the formation of which may be due to the reactions of the Li-rich $\text{LiCo}_{1/3}\text{Mn}_{1/3}\text{Ni}_{1/3}\text{O}_2$ thin film with air. The thickness of the film is estimated to be $0.6 \mu\text{m}$ after 2 h sputtering as shown in Fig. 2(b). Note that, apart from these islands, the film seems to be uniform, dense and crack free.

Fig. 3 shows the charge–discharge curves of the $\text{LiCo}_{1/3}\text{Mn}_{1/3}\text{Ni}_{1/3}\text{O}_2$ thin films on LATSP. Note that compared

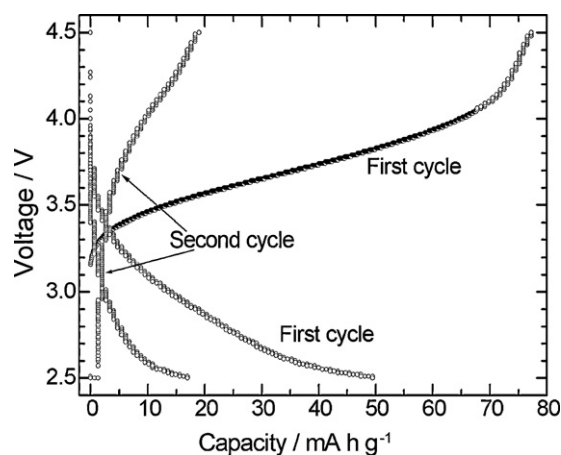


Fig. 5. Voltage profiles of the $\text{LiCo}_{1/3}\text{Mn}_{1/3}\text{Ni}_{1/3}\text{O}_2$ thin film on the solid electrolyte (LATSP) deposited in pure Ar. The curves were recorded between 2.5 and 4.5 V at a current density of $7.8 \mu\text{A cm}^{-2}$.

with the crystalline $\text{LiCo}_{1/3}\text{Mn}_{1/3}\text{Ni}_{1/3}\text{O}_2$ using liquid electrolyte [19], the as-deposited amorphous one shows a relatively low capacity. This is due to the fact that the $\text{LiCo}_{1/3}\text{Mn}_{1/3}\text{Ni}_{1/3}\text{O}_2$ thin film is conducting agent free and that the active area for electrochemical reactions is much smaller compared with the electrode in the liquid electrolyte. Nevertheless, a discharge capacity of around 130mAh g^{-1} is comparable to that of the well-crystallized LiCoO_2 . Furthermore, the irreversible capacity is not so significant for this thin amorphous film on LATSP. As a result, amorphous $\text{LiCo}_{1/3}\text{Mn}_{1/3}\text{Ni}_{1/3}\text{O}_2$ prepared at a low deposition temperature (below 130°C) seems to be a promising cathode material for all-solid-state Li-ion batteries, especially for microbatteries considering its practicable working voltage and specific capacity. As seen in Fig. 3(b), the capacity of the thin film is slightly increased by annealing at 500°C for 0.5 h. However, annealing will add the complexity of batteries preparation process and cause the undesired reactions between the deposited film and the electrolyte. Fig. 4 shows the Nyquist plots of the $\text{Li}/\text{PEO}_{18}\text{-Li}(\text{CF}_3\text{SO}_2)_2\text{N}/\text{LATSP}/\text{LiCo}_{1/3}\text{Mn}_{1/3}\text{Ni}_{1/3}\text{O}_2/\text{Au}$ cells. Note that the diameter of the semi-circles, which corresponds to the charge transfer resistance at the $\text{LiCo}_{1/3}\text{Mn}_{1/3}\text{Ni}_{1/3}\text{O}_2/\text{LATSP}$ interface, increases drastically with increasing the annealing temperature. In this regard, the low-temperature processing of thin film is favored.

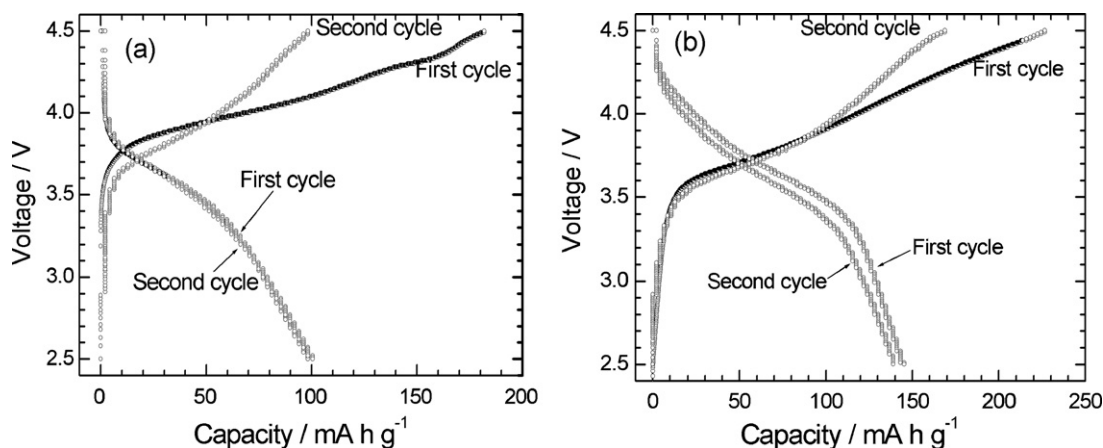


Fig. 6. Voltage profiles of (a) the as-deposited and (b) the 600°C -annealed $\text{LiCo}_{1/3}\text{Mn}_{1/3}\text{Ni}_{1/3}\text{O}_2$ thin films deposited on Au in Ar/O_2 (30% O_2). The curves were recorded between 2.5 and 4.5 V at a current density of $7.8 \mu\text{A cm}^{-2}$ using the liquid electrolyte.

Since the as-deposited film sputtered in pure Ar shows different microstructure as that in Ar+ 30% O₂ shown in Fig. 1, its electrochemical performance was also characterized. Fig. 5 shows the charge–discharge curves of the as-deposited film in pure Ar. Note that the film exhibits a rather poor electrochemical performance. This means the sputtering atmosphere plays an important role for the microstructure of the film.

Considering the fact that LiCo_{1/3}Mn_{1/3}Ni_{1/3}O₂ thin film is chemically stable with the Au substrate upon annealing, the electrochemical performance of the LiCo_{1/3}Mn_{1/3}Ni_{1/3}O₂ thin films deposited on the Au substrates in Ar/O₂ (30% O₂) was also checked using the liquid electrolyte. For the as-deposited film, a larger first irreversible capacity is evident compared with the film on LATSP as shown in Fig. 6(a). For the 600 °C-annealed sample on Au, a large irreversible capacity still exists as seen in Fig. 6(b). The obvious capacity increase after annealing is due to the improvement of the crystallization of the film. In addition, the film will crack after the high-temperature annealing. The cracking of the film will cause the penetration of the liquid electrolyte, also contributing to the increase of the capacity. For the LiCo_{1/3}Mn_{1/3}Ni_{1/3}O₂ thin film on LATSP, the capacity increase is caused mainly by the improved crystallization of the film since the solid electrolyte is used, excluding the penetration of the electrolyte. However, the capacity increase by annealing in the case of solid electrolyte is slight due to the formation of an inert layer at the LiCo_{1/3}Mn_{1/3}Ni_{1/3}O₂/LATSP interface during annealing, evidenced from the impedance profiles in Fig. 4, which makes it difficult for the charge transfer reactions occur. Therefore, for the fabrication of all-solid-state Li-ion batteries, the post-annealing temperature should be controlled as low as possible.

4. Conclusions

Amorphous LiCo_{1/3}Mn_{1/3}Ni_{1/3}O₂ thin films with a high operating voltage and a high specific capacity were prepared by RF magnetron sputtering in Ar/O₂ (30% O₂). A discharge capacity of around 130 mAh g⁻¹ is obtained for the amorphous film. The discharge capacity is slightly increased by annealing at 500 °C for 0.5 h, but the annealing also caused the interfacial reactions between LiCo_{1/3}Mn_{1/3}Ni_{1/3}O₂ and LATSP. The amorphous LiCo_{1/3}Mn_{1/3}Ni_{1/3}O₂ thin film prepared in pure Ar shows a poorer

electrochemical performance than that prepared in Ar/O₂ (30% O₂), even though it exhibits somewhat enhanced crystallization. The amorphous LiCo_{1/3}Mn_{1/3}Ni_{1/3}O₂ thin film on LATSP is considered to be a promising cathode for the all-solid-state microbatteries.

Acknowledgements

This research work was carried out under a collaboration program of Mie University and Genesis Research Institute, Nagoya, Japan. We thank OHARA Inc. for supplying the LATSP plates. We also thank the support of Zijin Program of Zhejiang University, China.

References

- [1] J.B. Bates, N.J. Dudney, G.R. Gruzalski, R.A. Zuhr, A. Choudhury, C.F. Luck, J.D. Robertson, *Solid State Ionics* 53–56 (1992) 647.
- [2] J.B. Bates, N.J. Dudney, G.R. Gruzalski, R.A. Zuhr, A. Choudhury, C.F. Luck, J.D. Robertson, *J. Power Sources* 43 (1993) 103.
- [3] X.H. Yu, J.B. Bates, G.E. Jellison Jr., F.X. Hart, *J. Electrochem. Soc.* 144 (1997) 524.
- [4] J. Fu, *Solid State Ionics* 96 (1997) 195.
- [5] J. Fu, *J. Am. Ceram. Soc.* 80 (1997) 1901.
- [6] J. Kawamura, N. Kuwata, K. Toribami, N. Sata, O. Kamishima, T. Hattori, *Solid State Ionics* 175 (2004) 273.
- [7] N. Kuwata, J. Kawamura, K. Toribami, T. Hattori, N. Sata, *Electrochem. Commun.* 6 (2004) 417.
- [8] Y. Inaguma, L.Q. Chen, M. Itoh, T. Nakamura, *Solid State Ionics* 70–71 (1994) 196.
- [9] M. Itoh, Y. Inaguma, W.H. Jung, L.Q. Chen, T. Nakamura, *Solid State Ionics* 70–71 (1994) 203.
- [10] K. Hoshina, K. Dokko, K. Kanamura, *J. Electrochem. Soc.* 152 (2005) A2138.
- [11] K. Dokko, K. Hoshina, H. Nakano, K. Kanamura, *J. Power Sources* 174 (2007) 1100.
- [12] J.F. Whitacre, W.C. West, E. Brandon, B.V. Ratnakumar, *J. Electrochem. Soc.* 148 (2001) A1078.
- [13] S.W. Jeon, J.K. Lim, S.H. Lim, S.M. Lee, *Electrochim. Acta* 51 (2005) 268.
- [14] Y. Iriyama, C. Yada, T. Abe, Z. Ogumi, K. Kikuchi, *Electrochem. Commun.* 8 (2006) 1287.
- [15] N. Kuwata, R. Kumar, K. Toribami, T. Suzuki, T. Hattori, J. Kawamura, *Solid State Ionics* 177 (2006) 2827.
- [16] J. Xie, N. Imanishi, T. Zhang, A. Hirano, Y. Takeda, O. Yamamoto, *J. Power Sources* 189 (2009) 365.
- [17] J. Xie, N. Imanishi, T. Zhang, A. Hirano, Y. Takeda, O. Yamamoto, *J. Power Sources* 192 (2009) 689.
- [18] Q. Li, H.Y. Sun, Y. Takeda, N. Imanishi, J. Yang, O. Yamamoto, *J. Power Sources* 94 (2001) 201.
- [19] T. Ohzuku, Y. Makimura, *Chem. Lett.* (2001) 642.
- [20] N. Yabuuchi, T. Ohzuku, *J. Power Sources* 119–121 (2003) 171.